DEUTSCHES ELEKTRONEN – SYNCHROTRON

DESY 93-017
March 1993

Search for Leptoquarks with the ZEUS Detector

ZEUS Collaboration

ISSN 0418-9833

NOTKESTRASSE 85 · D-2000 HAMBURG 52

To be sure that your preprints are promptly included in the
HIGH ENERGY PHYSICS INDEX,
send them to (if possible by air mail):

DESY **Bibliothek** **Notkestraße 85** **W-2000 Hamburg 52** **Germany**	**DESY-IfH** **Bibliothek** **Platanenallee 6** **O-1615 Zeuthen** **Germany**

DESY 93-017
March 1993

ISSN 0418-9833

Search for Leptoquarks with the ZEUS Detector

ZEUS Collaboration

March 9, 1993

Abstract

A search for any resonant state coupled to an electron and a proton constituent has been performed using collisions of electron and proton beams at HERA. In a sample with integrated luminosity of 26 nb^{-1}, no evidence has been found for production of leptoquarks with decays to $e^- + jet$ or $\nu + jet$. Limits on the coupling strength of scalar leptoquarks to electron and quark have been determined for masses above 25 GeV. For example, scalar isosinglet leptoquarks (S_0) with electroweak coupling strength to $(e^- u)$ states are ruled out at the 95% confidence level for masses below 168 GeV for left-handed couplings and below 176 GeV for right-handed couplings.

The ZEUS Collaboration

M. Derrick, D. Krakauer, S. Magill, B. Musgrave, J. Repond, S. Repond, R. Stanek, R.L. Talaga, J. Thron
Argonne National Laboratory, Argonne, IL, USA

F. Arzarello, R. Ayad[1], G. Bari, M. Basile, L. Bellagamba, D. Boscherini, A. Bruni, G. Bruni, P. Bruni, G. Cara Romeo, G. Castellini [2], M. Chiarini, L. Cifarelli, F. Cindolo, F. Ciralli, A. Contin, S. D'Auria, C. Del Papa, F. Frasconi, P. Giusti, G. Iacobucci, G. Laurenti, G. Levi, Q. Lin,B. Lisowski, G. Maccarrone, A. Margotti, T. Massam, R. Nania, C. Nemoz, F. Palmonari, G. Sartorelli, R. Timellini, Y. Zamora Garcia[1], A. Zichichi
University and INFN Bologna, Bologna, Italy

A. Bargende, J. Crittenden, H. Dabbous[3], K. Desch, B. Diekmann, T. Doeker, M. Geerts, G. Geitz, B. Gutjahr, H. Hartmann, J. Hartmann, D. Haun, K. Heinloth, E. Hilger, H.-P. Jakob, S. Kramarczyk, M. Kückes, A. Mass, S. Mengel, J. Mollen, D. Monaldi, H. Müsch, E. Paul, R. Schattevoy, J.-L. Schneider, R. Wedemeyer
Physikalisches Institut der Universität Bonn, Bonn, Federal Republic of Germany

A. Cassidy, D.G. Cussans, N. Dyce, H.F. Fawcett, B. Foster, R. Gilmore, G.P. Heath, M. Lancaster, T.J. Llewellyn, J. Malos, C.J.S. Morgado, R.J. Tapper, S.S. Wilson
Bristol University, Bristol, U.K.

R.R. Rau
Brookhaven National Laboratory, Upton, L.I., USA

M. Arneodo, T. Barillari, M. Schioppa, G. Susinno
Calabria University, Physics Dept.and INFN, Cosenza, Italy

A. Bernstein, A. Caldwell, I. Gialas, J.A. Parsons, S. Ritz, F. Sciulli[4], P.B. Straub, L. Wai, S. Yang
Columbia University, Nevis Labs., Irvington on Hudson,N.Y.,USA

J. Chwastowski[5], A. Dwuraźny, A. Eskreys, Z. Jakubowski[6], B. Nizioł, K. Piotrzkowski, M. Zachara, L. Zawiejski
Inst. of Nuclear Physics, Cracow, Poland

B. Bednarek, K. Eskreys, K. Jeleń, D. Kisielewska, T. Kowalski, E. Rulikowska-Zarębska, L. Suszycki, J. Zając
Faculty of Physics and Nuclear Techniques, Academy of Mining and Metallurgy, Cracow, Poland

T. Kędzierski, A. Kotański, M. Przybycień
Jagellonian Univ., Dept. of Physics, Cracow, Poland

L.A.T. Bauerdick, U. Behrens, J.K. Bienlein, C. Coldewey, A. Dannemann, G. Drews, P. Erhard[7], M. Flasiński[8], I. Fleck, A. Fürtjes, R. Gläser[9], P. Göttlicher, T. Haas, L. Hagge, W. Hain, D. Hasell, H. Hultschig, G. Jahnen[10], P. Joos, M. Kasemann, R. Klanner, W. Koch, U. Kötz, H. Kowalski, J. Labs, A. Ladage, B. Löhr, M. Löwe, D. Lüke, J. Mainusch, O. Manczak[11], M. Momayezi, J.S.T. Ng, S. Nickel, D. Notz, I.H. Park, K.-U. Pösnecker[12], M. Rohde, J. Roldán[13], E. Ros[5], U. Schneekloth, J. Schroeder, W. Schulz, F. Selonke, E. Stiliaris[13], E. Tscheslog[14], T. Tsurugai, F. Turkot[15], W. Vogel[16], G. Wolf, C. Youngman
Deutsches Elektronen-Synchrotron DESY, Hamburg, Federal Republic of Germany

H.J. Grabosch, A. Leich, A. Meyer, C. Rethfeldt, S. Schlenstedt
DESY-Zeuthen, Inst. für Hochenergiephysik, Zeuthen, Federal Republic of Germany

G. Barbagli, A. Francescato, M. Nuti, P. Pelfer
University and INFN, Florence, Italy

G. Anzivino, R. Casaccia, S. De Pasquale, S. Qian, L. Votano
INFN, Laboratori Nazionali di Frascati, Frascati, Italy

A. Bamberger, A. Freidhof, T. Poser, S. Söldner-Rembold, G. Theisen, T. Trefzger
Physikalisches Institut der Universität Freiburg, Freiburg, Federal Republic of Germany

N.H. Brook, P.J. Bussey, A.T. Doyle, J.R. Forbes, V.A. Jamieson, C. Raine, D.H. Saxon
Dept. of Physics and Astronomy, University of Glasgow, Glasgow, U.K.

H. Brückmann[17], G. Gloth, U. Holm, H. Kammerlocher, B. Krebs, T. Neumann, K. Wick
Hamburg University, I. Institute of Exp. Physics, Hamburg, Federal Republic of Germany

A. Fürtjes, W. Kröger, E. Lohrmann, J. Milewski[11], M. Nakahata, N. Pavel, G. Poelz, A. Seidman[18], W. Schott, J. Terron[13], B.H. Wiik, F. Zetsche
Hamburg University, II. Institute of Exp. Physics, Hamburg, Federal Republic of Germany

T.C. Bacon, I. Butterworth, C. Markou, D. McQuillan, D.B. Miller, M.M. Mobayyen, A. Prinias, A. Vorvolakos
Imperial College London, High Energy Nuclear Physics Group, London, U.K.

T. Bienz, H. Kreutzmann, U. Mallik, E. McCliment, M. Roco, M.Z. Wang
University of Iowa, Physics and Astronomy Dept., Iowa City, USA

P. Cloth, D. Filges
Forschungszentrum Jülich, Institut für Kernphysik, Jülich, Federal Republic of Germany

L. Chen, R. Imlay, S. Kartik, H.-J. Kim, R.R. McNeil, W. Metcalf
Louisiana State University, Dept. of Physics and Astronomy, Baton Rouge, LA, USA

F. Barreiro[19], G. Cases, L. Hervás[20], L. Labarga[20], J. del Peso, J.F. de Trocóniz[21]
Univer. Autónoma Madrid, Depto de Física Teórica, Madrid, Spain

F. Ikraiam, J.K. Mayer, G.R. Smith
University of Manitoba, Dept. of Physics, Winnipeg, Manitoba, Canada

F. Corriveau, D.J. Gilkinson, D.S. Hanna[4], L.W. Hung, J.W. Mitchell, P.M. Patel, L.E. Sinclair, D.G. Stairs, R. Ullmann
McGill University, Dept. of Physics, Montreal, Quebec, Canada

G.L. Bashindzhagyan, P.F. Ermolov, Y.A. Golubkov, V.A. Kuzmin, E.N. Kuznetsov, A.A. Savin, A.G. Voronin, N.P. Zotov
Moscow State University, Institute of Nuclear Pysics, Moscow, Russia

S. Bentvelsen, M. Botje, A. Dake, J. Engelen, P. de Jong, M. de Kamps, P. Kooijman, A. Kruse, H. van der Lugt, V. O'Dell, A. Tenner, H. Tiecke, J. Vermeulen, M. Vreeswijk, L. Wiggers, E. de Wolf, R. van Woudenberg, R. Yoshida
NIKHEF-Amsterdam, Netherlands

B. Bylsma, L.S. Durkin, C. Li, T.Y. Ling, K.W. McLean, W.N. Murray, S.K. Park, T.A. Romanowski[22], R. Seidlein
Ohio State University, Physics Department, Columbus, Ohio, USA

G.A. Blair, J.M. Butterworth, A. Byrne, R.J. Cashmore, A.M. Cooper-Sarkar, R.C.E. Devenish, D.M. Gingrich[23], P.M. Hallam-Baker[6], N. Harnew, T. Khatri, K.R. Long, P. Luffman, I. McArthur, P. Morawitz, J. Nash, S.J.P. Smith[24], N.C. Roocroft, F.F. Wilson
Department of Physics, University of Oxford, Oxford, U.K.

G. Abbiendi, R. Brugnera, R. Carlin, F. Dal Corso, M. De Giorgi, U. Dosselli, F. Gasparini, S. Limentani, M. Morandin, M. Posocco, L. Stanco, R. Stroili, C. Voci
Dipartimento di Fisica dell' Universita and INFN, Padova, Italy

G. Feild, J.N. Lim, B.Y. Oh[25], J. Whitmore[26]
Pennsylvania State University, Dept. of Physics, University Park, PA, USA

U. Contino, G. D'Agostini, M. Guida[27], M. Iori, S.M. Mari, G. Marini, M. Mattioli, A. Nigro
Dipartimento di Fisica, Univ. 'La Sapienza' and INFN, Rome, Italy

J.C. Hart, N.A. McCubbin, K. Prytz, T.P. Shah, T.L. Short
Rutherford Appleton Laboratory, Chilton, Didcot, Ozon, U.K.

E. Barberis, N. Cartiglia, C. Heusch, B. Hubbard, J. Leslie, W. Lockman, K. O'Shaughnessy, H.F. Sadrozinski, A. Seiden
University of California, Santa Cruz, CA, USA

E. Badura, J. Biltzinger, H. Chaves, M. Rost, R.J. Seifert, A.H. Walenta, W. Weihs, G. Zech
Fachbereich Physik der Universität-Gesamthochschule Siegen, Federal Republic of Germany

S. Dagan[28], A. Levy, D. Zer-Zion
School of Physics, Tel-Aviv University, Tel Aviv, Israel

T. Hasegawa, M. Hazumi, T. Ishii, S. Kasai[29], M. Kuze, Y. Nagasawa, M. Nakao, H. Okuno, K. Tokushuku, T. Watanabe, S. Yamada
Institute for Nuclear Study, University of Tokyo, Tokyo, Japan

M. Chiba, R. Hamatsu, T. Hirose, S. Kitamura, S. Nagayama, Y. Nakamitsu
Tokyo Metropolitan University, Dept. of Physics, Tokyo, Japan

R. Cirio, M. Costa, M.I. Ferrero, L. Lamberti, S. Maselli, C. Peroni, A. Solano, A. Staiano
Universita di Torino, Dipartimento di Fisica Sperimentale and INFN, Torino, Italy

M. Dardo
Universita di Torino, Facultá di Scienze MFN and INFN, Alessandria, Italy

D.C. Bailey, D. Bandyopadhyay, F. Benard, S. Bhadra, M. Brkic, B.D. Burow, F.S. Chlebana, M.B. Crombie, G.F. Hartner, G.M. Levman, J.F. Martin, R.S. Orr, J.D. Prentice, C.R. Sampson, G.G. Stairs, R.J. Teuscher, T.-S. Yoon
University of Toronto, Dept. of Physics, Toronto, Ont., Canada

F.W. Bullock, C.D. Catterall, J.C. Giddings, T.W. Jones, A.M. Khan, J.B. Lane, P.L. Makkar, D. Shaw, J. Shulman
University College London, Physics and Astronomy Dept., London, U.K.

K. Blankenship, D.B. Gibaut, J. Kochocki, B. Lu, L.W. Mo
Virginia Polytechnic Inst. and State University, Physics Dept., Blacksburg, VA, USA

K. Charchuła, J. Ciborowski, J. Gajewski, G. Grzelak, M. Kasprzak, M. Krzyżanowski, K. Muchorowski, R.J. Nowak, J.M. Pawlak, A. Stopczyński, T. Tymieniecka, R. Walczak, A.K. Wróblewski, J.A. Zakrzewski, A.F. Żarnecki
Warsaw University, Institute of Experimental Physics, Warsaw, Poland

M. Adamus
Institute for Nuclear Studies, Warsaw, Poland

H. Abramowicz[11], Y. Eisenberg, C. Glasman[30], U. Karshon[28], A. Montag[28], D. Revel, A. Shapira
Weizmann Institute, Nuclear Physics Dept., Rehovot, Israel

C. Foudas, C. Fordham, R.J. Loveless, A. Goussiou, I. Ali, B. Behrens, S. Dasu, D.D. Reeder, W.H. Smith, S. Silverstein
University of Wisconsin, Dept. of Physics, Madison, WI, USA

W.R. Frisken, K.M. Furutani, Y. Iga
York University, Dept. of Physics, North York, Ont., Canada

[1] supported by Worldlab, Lausanne, Switzerland
[2] also at IROE Florence, Italy
[3] now a self-employed consultant
[4] now at DESY as Alexander von Humboldt Fellow
[5] now at CERN
[6] now at DESY
[7] now at IST GmbH, Darmstadt
[8] on leave from Jagellonian University, Cracow
[9] now at Martin & Associates, Hamburg
[10] now at Harry Hoffmann, Fitzbek
[11] on leave from Warsaw University, Warsaw
[12] now at Lufthansa, Frankfurt
[13] supported by the European Community
[14] now at Integrata, Frankfurt
[15] on leave from FERMILAB
[16] now at Blohm & Voss, Hamburg
[17] deceased
[18] on leave from Tel Aviv, University supported by DFG
[19] on leave of absence at DESY, supported by DGICYT
[20] partially supported by Comunidad Autónoma de Madrid, Spain
[21] supported by Fundación Banco Exterior
[22] now at Department of Energy, Washington
[23] now at Centre for Subatomic Research, Univ.of Alberta, Canada and TRIUMF, Vancouver, Canada
[24] now with McKinsey Consultants, Sidney, Australia
[25] on leave and supported by DESY 1992-93
[26] on leave and supported by DESY 1991-92
[27] permanent address Dip. di Fisica, Univ. di Salerno, Italy
[28] supported by the MINERVA Gesellschaft für Forschung GmbH
[29] now at Hiroshima National College of Maritime Technology
[30] supported by the DAAD - Deutscher akademischer Austauschdienst

1 Introduction

In the standard model of elementary particles, leptons and quarks interact with each other only through electroweak forces. New lepton-quark forces could result in leptoquark states (LQ) coupled to leptons and quarks that are not predicted in the standard model. For example, point-like leptoquarks in many extensions of the standard model [1] mediate new forces between quarks and leptons. A set of such elementary bosons has been compiled [2, 3] and constraints on various leptoquark couplings have been estimated [4] under specific assumptions from low energy measurements and from the equality of the weak constants in β-decay and muon decay.

Leptoquark pair-production has been sought in experiments at e^+e^- and hadron-hadron colliders. Their production relies on the coupling of Z^0 to the leptoquark pairs via electroweak charge for e^+e^- and on the coupling of gluons to the leptoquark pairs via color for hadron colliders. Hence, such collider experiments do not depend on the leptoquark coupling to lepton and quark but may be sensitive to other properties of the leptoquark state, such as spatial extent or additional couplings. Experiments from LEP [5] limit elementary leptoquarks to masses above 44 GeV for any branching fraction, b, for decay to $e+jet$. Comparable limits are quoted by UA2 for $b = 0.12$, but extend to a mass of 74 GeV for $b = 1$ [6]. CDF limits [7] from 45 to 113 GeV have been reported for b from 0.1 to 1.0.

The electron-proton collider, HERA, permits a natural and complementary technique in that a single leptoquark state may be produced. Here the production depends directly on the lepton-quark coupling to the leptoquark, and does not depend on other couplings or on the size of the LQ state. Preliminary results have been presented by H1 and ZEUS on this question [8]. In this experiment, the ZEUS collaboration used data taken from collisions of 820 GeV protons with 26.7 GeV electrons. Evidence was sought for leptoquarks in a selected sample of 1659 neutral current and 2 charged current candidate events corresponding to an integrated luminosity of 26 nb^{-1}.

2 Production and Decay of Scalar Leptoquarks

At HERA, any state coupled to an electron and a proton constituent will be formed as a resonance in the s-channel if there is adequate energy to produce it. Take as one example a spin zero leptoquark of mass, M_{LQ}, coupled to e^- and u. Such a state is produced with a Breit-Wigner amplitude which peaks at $\hat{s} = M_{LQ}^2$, where $\hat{s}$ is the square of the center-of-mass energy between the incident electron and the struck quark. Since the fractional momentum of this quark is given by the Bjorken x-variable, then $\hat{s} = xs$. Hence, with the ep center-of-mass energy ($\sqrt{s} = 296$ GeV) fixed by the collider beam energies, production and decay of a leptoquark state will be signaled by a resonant peak in the x-distribution of neutral current type (NC) events

$$e^- + p \rightarrow e^- + X \tag{1}$$

at

$$x_0 = \frac{M_{LQ}^2}{s}. \tag{2}$$

The dominant contribution to the cross-section over regions of interest for reaction 1 at $x \neq x_0$ is from deep-inelastic scattering (DIS) involving vector-boson exchange. Other terms, including cross-channel leptoquark exchange, are small for the masses and couplings discussed here. The total cross-section [2] for LQ production, for small resonant widths and ignoring radiative corrections and DIS-LQ interference, is

$$\sigma = \frac{\pi}{4s} g^2 u(x_0, \mu) \tag{3}$$

where $u(x_0, \mu)$ is the probability density for finding a u-quark at $x = x_0$; the scale, μ, is taken to be $\mu = M_{LQ}$. The coupling, $g = \sqrt{g_R^2 + g_L^2}$, is composed of the left-handed (g_L) and right-handed (g_R) couplings at the electron-quark-leptoquark vertex. More generally, equation (3) applies in the narrow width approximation for any spin-0 resonant state of electron and quark (or anti-quark) by substitution of the appropriate parton density for $u(x_0, \mu)$. (We take the coupling as either left- or right-handed: $g_R = 0$ or $g_L = 0$.) Though these couplings are completely unspecified in the general case, the usual reference value for g_L or g_R is $\sqrt{4\pi\alpha_{EW}} \approx 0.31$ at $\mu = M_{LQ}$. The width of the leptoquark (per decay channel) for this "electroweak" coupling is $\Gamma \approx 0.002 M_{LQ}$. Over the range of masses and couplings discussed here, intrinsic widths for produced leptoquarks are small compared to experimental resolutions. Conversely, widths are large enough so that leptoquarks decay promptly in the experimental apparatus.

Flavor-conserving leptoquarks with left-handed coupling of appropriate electric charge decay to the final state (1) but may also decay to the final state typical of charged current (CC) processes:

$$e^- + p \rightarrow \nu_e + X. \tag{4}$$

We denote the branching fraction for LQ decay to (1) as $b = \Gamma_{NC}/(\Gamma_{NC} + \Gamma_{CC})$. Scalar e^--induced leptoquarks with right-handed coupling or with left-handed coupling and electric charge, $q \neq -\frac{1}{3}$, are forbidden to decay into the CC final state (4), so $b = 1$ for such states. (See table 3).

The scaling variable y is related to the decay polar angle, θ^*, in the LQ rest frame by $1 - y = (1 + \cos\theta^*)/2$. The y-dependence of the leptoquark cross-section is a direct consequence of the leptoquark spin. For the scalar case taken here, the cross-section is independent of y.

The major backgrounds to a leptoquark resonance arise from the DIS continuum. The NC background from DIS is dominated by photon exchange and so gives a rate proportional to $1/Q^4 = 1/s^2x^2y^2$. At fixed x, this rate falls quickly with y whereas leptoquarks will give a much flatter y-dependence. Removing NC events at small y discards a large fraction of the DIS continuum with relatively small penalty to a leptoquark signal. This is also true after inclusion of radiative effects. For our integrated luminosity, the CC background is expected to be small (1.1 events after all selections).

The LQ search region extended from masses of 25 (50) GeV up to the kinematic limit for the event samples corresponding to reactions (1) and (4), respectively.

3 Data Taking and Simulation

The ZEUS detector has been described in several recent publications [9, 10, 11]. The large solid angle precision calorimeter, the central tracking detector, and the luminosity monitor

(LUMI) were the principal components used for this analysis. The calorimeter consists of three structures: FCAL, in the direction of the proton beam ($\theta = 0°$); BCAL, covering the central region; and RCAL, in the direction of the electron beam ($\theta = 180°$). The calorimeter readout [12] provided energy [13, 14] and time with high precision and low noise for each of the 5918 cells instrumented with two photomultipliers (PMT) on each cell. For the tracking, only coarse trigger information [15] from the central tracking detector (CTD) was used for this analysis. The LUMI detectors measured final state electrons and photons in the direction of the incident electron beam, both to provide a luminosity measurement from bremsstrahlung events, and to provide information for analysis of events with coincident e's and γ's.

Data were accumulated while HERA operated with 9 colliding electron and proton bunches; single additional unpaired "pilot" bunches of electrons and protons permitted estimation of beam-associated backgrounds. The vertex distribution along the beam direction had $\sigma_z \approx 25$ cm r.m.s. originating from the proton bunch length. Triggering of data utilized sums over calorimeter cells [9], the most important of which were electromagnetic towers with typical thresholds of 2.5 GeV. The trigger acceptance for LQ decaying into the NC final states (1), as estimated from Monte Carlo trigger simulation, was greater than 99%. The trigger acceptance for decays into CC final states (4) was greater than 79% over the search range.

The kinematic quantities x, y, and Q^2 were determined from measurements of calorimeter energies. The algorithms [16] to evaluate all variables were described in more detail in a previous publication [9]. For y, the Jacquet-Blondel algorithm which uses only hadronic quantities was used (y_{JB}); for Q^2, electron measurements were employed for NC and hadronic measurements for CC; for x, the double-angle method "x_{DA}" was used for NC events and "x_{JB}" for CC events. It should be noted that x_{DA} depends little on overall energy calibration.

Simulation of leptoquarks and calculation of LQ production cross-sections were accomplished using the Monte Carlo program PYTHIA [17] assuming electroweak coupling, with MTB1 parton densities [18] and including radiative corrections. Interference between DIS and LQ amplitudes was not included and will be discussed in the section on results. Over the kinematic regions of importance, the Born cross-sections agree well with calculations from the generator LQUARK [19] with the same assumptions.

Monte Carlo simulation of the detector was accomplished for both DIS and LQ configurations using MOZART, the ZEUS simulation in GEANT 3.13 [20]. The response of the calorimeter measured with test-beams [13, 14] was used to set parameters and to check the validity of the simulation. At present, we estimate from comparisons with data that the simulation systematically reproduces energies to about 5%. Monte Carlo events and data events were processed through identical selection and analysis chains.

4 Fiducial Sample Selection

The triggered sample of about four million candidates was subjected to a series of cuts whose purpose was to separate DIS events from other backgrounds and to provide a NC fiducial sample for studies of non-DIS backgrounds and for validation of Monte Carlo calculated LQ efficiencies. Quantities used to select NC and CC events are (a) the net (or missing) transverse momentum in the event, p_T, which should be zero for NC events and non-zero for CC events due to the undetected final state neutrino; and (b) the longitudinal energy variable, $\delta = \sum E_i(1 - \cos\theta_i)$,

Table 1: Cuts for Fiducial and Final Candidate Samples

Selection	$NC: e+jet$	$CC: \nu+jet$
Preselection	20491	7579
$E_{lumi} < 5\ GeV$	16955	7508
ep bunch	16670	6507
Final timing	16548	6369
Good vertex	12369	751
e^- found: $E_e > 10\ GeV$	4500	—
p_T conserved	4496	—
Fiducial Samples	4496	751
$30 < \delta < 60\ GeV$	4260	—
$y_{JB} > 0.1$	1659	—
cone cut: $p_T > 10\ GeV$	—	23
$y_{JB} < 1$	1659	12
CC scan	—	2
LQ Search Samples	1659	2

obtained as a sum over all calorimeter cells with energies, E_i, and angles, θ_i, relative to the interaction point. The value of δ should be near twice the electron beam energy for NC events and less than this value for CC events.

The initial selection for NC-type events required that an isolated electron candidate be found and that $\delta > 20\ GeV$. The fraction of the candidates that satisfied these requirements increased as the machine luminosity and trigger discrimination improved, ranging from 3% during early running to 12% at the end. For the CC selection, events were required to have $p_T > 10\ GeV$. Approximately 2% of the triggers satisfied this requirement.

Both NC and CC samples were subjected to further cuts that removed events with topologies of cosmic ray showers and false triggers resulting from single large PMT pulses. Calorimeter timing requirements removed interactions of protons inside the beam pipe upstream of the detector. The procedure, similar to that described previously for a subset of this data [9], further reduced the samples by more than an order of magnitude. Timing distributions at this and subsequent stages showed that these cuts were conservatively larger than the timing resolutions ($\approx 1\ ns$). These pre-selections provided 20491 NC candidates and 7579 CC candidates.

Table 1 shows the effects of subsequent cuts on these samples. Photoproduction backgrounds contain events with a recoil electron that misses RCAL. An electron in the electron beam direction may be signalled by a coincident energy deposition in the electron arm of the LUMI detector. A cut on the LUMI electron energy, $E_{lumi} < 5\ GeV$, was imposed. Events were then required to occur in one of the nine matching RF-bunches with electrons and protons. Tighter timing cuts further reduced the samples slightly and removed additional beam-associated backgrounds.

The events were required to have a good vertex, defined as having at least one good track pointing to within 8 cm of the beam line and beam coordinate, z, within 75 cm of the nominal interaction point from at least one of two tracking algorithms. This cut substantially reduced both the NC and CC samples; the efficiency of this procedure for leptoquarks will be addressed later. All subsequent calculations of kinematic quantities use z and the transverse coordinates of the beam line as the interaction vertex position.

Two additional cuts specific to the NC sample are shown in table 1. The first utilized an electron-finding algorithm based solely on the spatial energy deposition compared to that characteristic of isolated electrons. The process used the characteristics of electron and hadron showers from test beam data [13, 14], allowing for somewhat larger transverse sizes of electron showers expected due to material in front of the calorimeter. Electron finding did not require a reconstructed track in the CTD. The electron energy was required to be greater than 10 GeV; this substantially reduced background from photoproduction while having a negligible effect on the efficiency for LQ decays with $M_{LQ} > 50\ GeV$. Finally, a "fiducial NC sample" of 4496 events was specified by requiring p_T less than the larger of 10 GeV or $2\sqrt{E_T}\ GeV$, where E_T is the total transverse energy in GeV.

The backgrounds to LQ production from processes other than DIS in the fiducial NC sample are small. Events induced by cosmic ray interactions or from false calorimeter triggers are obvious from visual examination of event displays. The fraction of such background in the sample, determined by a scan of a subset, is found to be less than 0.1 % (90% CL).

To test for false events triggered by proton beam interactions with stationary targets (such as gas) in the beampipe, the selections in table 1 were repeated with the "ep bunch" selection replaced by em requiring events from the unpaired proton pilot bunch. No event survived this selection, implying that this background constitutes less than 0.5% (90% CL) of the fiducial NC sample. In a similar manner, background from electron beam interactions with stationary targets is estimated from events in the electron pilot bunch to be (0.6 ± 0.3)%.

Other than DIS, the largest expected background is from low Q^2 photoproduction processes in which the final state electron misses the calorimeter and a false electron is found in the debris of a hadron shower. (Such false electrons are most likely to come from decays of $\pi^0 \rightarrow \gamma + \gamma$.) Monte Carlo studies [9] indicate that about one-quarter of photoproduction events will have an electron tagged by the LUMI detector. This fraction is consistent with that obtained from analysis of hard photoproduction processes [10]. The selection for the NC fiducial sample was repeated, replacing the $E_{lumi} < 5\ GeV$ requirement with $E_{lumi} > 5\ GeV$; that is, requiring the presence of an electron. The 91 observed events permitted an estimate of (3.5 ± 2.5)% for the photoproduction background in the fiducial NC sample. This background level would be a problem only if such events were to preferentially populate large x.

Indeed, a dangerous potential background for leptoquark searches comes from processes, like photoproduction, that may contain false wide angle electrons which in turn may produce false large values of x (or M_{LQ}). Since such backgrounds arise largely from photon conversions, they will have no associated charged track in the CTD. The 944 events of the fiducial sample with wide angle electrons ($10° \lesssim \theta_e \lesssim 170°$) were examined using the CTD, which had not been used in the electron finding algorithm. The 11 events without evidence for a charged track provided an independent estimate of the background fraction for false wide angle electron events of (1.2 ± 0.4)%. This demonstrates that backgrounds other than DIS do not preferentially populate the large x region.

5 Detection Efficiency Studies

Neutral current DIS events have predominantly small Q^2 (θ_e near 180°) and so have a different topology compared to the wide electron and jet angles characteristic of LQ decays. The vertex requirement was essential for rejection of backgrounds and for good mass resolution. To confirm that the Monte Carlo calculation of vertex-finding efficiency was valid, the data selection was repeated without the vertex requirement, but requiring some energy deposition in the FCAL ($> 1\ GeV$) to keep backgrounds small. The fraction of these events with a reconstructed vertex was determined, and the process was repeated for the Monte Carlo DIS events. The efficiency obtained in this way for the data was $\epsilon_{tot} = 0.66$; that determined by the Monte Carlo calculation agreed within 1%. More importantly, only six of the 60 data events with electron angles in the range ($37° < \theta_e < 143°$) were found to have a missed vertex, in quantitative agreement with the Monte Carlo prediction of 4.8 missed vertex events with these wide angles.

The sample of 933 events with validated electrons (described in the previous section) was further checked to corroborate whether events with a wide angle electron had a well-determined electron track. For the 152 events with $\theta_e < 154°$, the efficiency for finding an electron track was $\epsilon_{trk} = 0.95 \pm 0.02$. This high value gives confidence that the efficiency of the tracking and vertex reconstruction for LQ decays through the NC mode, in which both a wide angle electron and additional hadrons are typically present, is high.

In order to corroborate that the vertex finding efficiency for CC events was properly simulated, the fraction of events with multi-track vertices in the fiducial NC sample was calculated. From one tracking algorithm, this fraction (79%) was about 4% less than the Monte Carlo estimate; for the other algorithm, the data fraction (87%) was larger than the Monte Carlo calculation by about 5%. We conclude that the simulation of vertex efficiency for CC decays of LQ and for CC events is adequately represented by the simulation.

6 Final Leptoquark Selection

Subsequent cuts to isolate an LQ signal in the NC sample are shown in table 1. The requirement for δ to lie within conservative limits removes more photoproduction background. The cut on y_{JB} removes a substantial fraction of the low Q^2 DIS events, as described earlier. The final sample for the LQ search consisted of 1659 events, dominated by DIS, with other backgrounds at the small fractional levels similar to those of the fiducial NC sample discussed previously.

Figure 1 shows the x_{DA}-distribution of the 465 events with $x_{DA} > 0.001$ for this final NC sample (circles) compared with the Monte Carlo prediction. The predicted rate (unshaded dashed histogram) is normalized to the data luminosity, $\int \mathcal{L} dt = (26.0 \pm 2.6)\ nb^{-1}$. The figure indicates that the agreement with the Monte Carlo prediction, using MTB1 structure functions [18], is reasonable for $x_{DA} > 0.01$, where measurements of structure functions exist at lower energies and the acceptance of the ZEUS detector is high.

The 751 CC candidates remaining after the vertex requirement were found to consist primarily of halo protons or secondaries interacting in a collimator adjacent to the FCAL. These interactions asymmetrically deposited large amounts of energy in the FCAL near the beam pipe, resulting in triggers with unbalanced transverse momentum, but with energy deposits at small

Table 2: Charged Current Event Candidates

Variable	Event A	Event B
$p_T(\ GeV)$	14 ± 3	94 ± 11
x	0.014 ± 0.003	0.44 ± 0.09
y	0.20 ± 0.05	0.35 ± 0.12
$Q^2\ (GeV^2)$	245 ± 70	14000 ± 3000

angles. A procedure which is largely independent of the details of fragmentation was devised to select CC candidates with good efficiency. This involved a recalculation of the net p_T for each candidate, using the vertex, and ignoring all energy within a cone of 13.8° in the FCAL adjacent to the beam pipe. Imposing the transverse momentum selection with this algorithm (cone cut) reduced the sample to 23 events. The reduction in efficiency for detection of leptoquarks of mass $M_{LQ} = 150\ GeV$ resulting from application of the cone algorithm was about 3%. Furthermore, it was verified from the NC fiducial sample that the small shifts in calculated p_T created by the cone cut were well described by the Monte Carlo simulation.

Of the 23 remaining CC candidates, the 11 events with unphysical values of the y-variable ($y > 1$) were removed. On examination, all of these proved to be background. The remaining 12 events were scanned; 7 were found to have been induced by cosmic rays, 2 were from interactions of the proton beam upstream of the detector, 1 was a NC event with a well-identified electron in the final state but with the vertex wrongly reconstructed, 1 was a candidate CC event (event A) and 1 event was a clear CC event (event B) with the interesting characteristics shown in table 2.

Both events A and B were retained for the purposes of the LQ search. The number of CC events from DIS mechanisms expected for the measured luminosity after all cuts is 1.1 events, consistent with the number observed.

7 Results

The data of fig. 1 and of table 2 give no significant indication for leptoquark production and decay. We therefore establish limits on the cross-section and couplings for leptoquark production and decay to $e + jet$ (1) and $\nu + jet$ (4).

For LQ $\rightarrow\ e + jet$ (NC mode), efficiencies and reconstructed quantities were calculated using samples of 1000 Monte Carlo events at each of 10 different mass values. Measured variables were calculated and triggering/filtering cuts were applied in a manner identical to the data. An example of the reconstructed distribution of x_{DA} for events expected for electroweak coupling with $M_{LQ} = 150\ GeV$ is shown as shaded histograms in fig. 1. Such distributions were fit in the peak region with a Gaussian function to obtain a mean (μ_x) and standard deviation (σ_x) for x_{DA}. The overall efficiency, including triggering, all cuts, and the probability to be within $\pm 3\sigma_x$ of μ_x was evaluated. This efficiency was between 40% and 60% over the LQ mass search range of 25 to 220 GeV. The requirement of an isolated electron and the cut $y > 0.1$ account for about 20% of the inefficiency.

For LQ $\rightarrow \nu + jet$ (CC mode), a similar procedure was followed with one important difference. The search variable, x_{JB}, had typical resolution a factor two larger than the NC case in which x_{DA} was used and for which $\sigma_x \approx 0.1\mu_x$. The overall efficiency was between 65% and 75% over the CC search range.

At each candidate mass, the search region ($\mu_x \pm 3\sigma_x$) was specified from the simulation. Within this region the number of data events was counted, and the number of background events was obtained from the DIS Monte Carlo simulation normalized to the measured luminosity (which agrees with the observed DIS data). These values were used to determine the number of LQ events to which the experiment was sensitive at the 95% confidence level (CL) using the expression for Poisson probability limits in the presence of background [21]. This number of events, divided by efficiency and measured luminosity, provides the sensitive cross-section at the same confidence level. These limits on cross-section time branching ratio are given as a function of leptoquark mass in the appendix. The coupling limit then follows from the cross-sections, evaluated with PYTHIA at electroweak coupling, and scaled to different couplings at the same mass using equation (3).

Figure 2 shows the 95% confidence limits on coupling constant versus M_{LQ} for scalar isosinglet leptoquarks (S_0) with (e^-u) quantum numbers for (a) right-handed coupling; and (b) left-handed coupling. In the former case, only the neutral current data contribute; in the latter case, limits are shown from neutral current data (dotted) and from charged current data (dashed) assuming the branching fraction to each equals $\frac{1}{2}$. Note that the sensitivity is comparable for the two decay modes at high masses. The solid curve shows the limit for the combined NC and CC data also for $b = \frac{1}{2}$. At high masses the limit would be similar for any branching fraction.

The uncertainties in this procedure include those due to luminosity (10%) and to LQ inefficiency, ϵ. We estimate the latter to be $\sigma_\epsilon = 0.1\epsilon$. Together these create uncertainties in the limit on g of fig. 2 of $\pm 7\%$. If these normalization errors are treated as random Gaussian errors for calculation of probability, the systematic shift in the limit on g is less than 1.5% upward.

For convenience of calculation, the terms due to interference between DIS and LQ production have been ignored. Such terms generally increase the cross-section; if they were included, the limits on g would shift downward by less than 1% at lower masses and downward by about 3% at $M_{LQ} = 200\ GeV$.

Finally, the set of structure functions used to calculate the curves of fig. 2 (MTB1) is but one of a large group of such phenomenological fits. Comparison with the MRSD0 structure functions [22], for example, indicates that the limits on g could change by -8% to $+4\%$ over the range of masses from 25 to 225 GeV. Different scale assumptions ($\mu \approx Q\ vs\ M_{LQ}$) have a negligible effect.

Limits were obtained for other leptoquark types by employing appropriate quark densities in expressions analogous to equation (3). Table 3 gives the mass limits, assuming electroweak coupling, for various scalar leptoquarks catalogued with invariant $SU(3) \times SU(2) \times U(1)$ couplings [2, 3]. The columns provide the charge (q), fermion number (F), weak isospin (I_{wk}), and the flavor. Mass degeneracy is assumed for charge multiplets. For those LQ which can decay into both NC and CC modes, the table assumes equal branching fractions (b), but the limit is within 2 GeV of that tabulated for any branching fraction.

Table 3: Mass Limits (GeV) on Scalar Leptoquarks for $g = 0.31$ at 95% CL

LQ				Left-handed			Right-handed		
Type	q	F	I_{wk}	Quark	b	Limit	Quark	b	Limit
S_0	$-\frac{1}{3}$	-2	0	u	$\frac{1}{2}$	168	u	1	176
$\tilde{S}_0$	$-\frac{4}{3}$	-2	0	—	—	—	d	1	146
S_1	$-\frac{1}{3}$,$-\frac{4}{3}$	-2	1	u, d	$\frac{1}{2}$,1	184	—	—	—
$S_{1/2}$	$-\frac{5}{3}$,$-\frac{2}{3}$	0	$\frac{1}{2}$	$\bar{u}$,–	1,–	92	$\bar{u}, \bar{d}$	1	108
$\tilde{S}_{1/2}$	$-\frac{2}{3}$	0	$\frac{1}{2}$	$\bar{d}$	1	92	—	—	—

8 Conclusions

This leptoquark search, with an integrated luminosity of 26 nb^{-1}, utilized selected samples of 1659 $e + jet$ (NC) and two $\nu + jet$ (CC) event candidates. These samples, consistent with deep inelastic mechanisms, show no significant indication of a leptoquark resonance.

Monte Carlo studies indicate that the efficiency for selecting the high transverse momentum final states of LQ decay is typically 50% (70%) for NC (CC) final states. Various redundant checks on the triggering and selections were applied to a fiducial sample of 4496 NC events.

Figure 2 shows the limits at 95% confidence of LQ-electron-quark coupling for the (e^-u) LQ decay to NC and CC final states. The combined limit on left-handed coupling is largely independent of decay mode for $M_{LQ} > 160\ GeV$. For coupling equal to that of electroweak interactions, the mass limits for left-handed coupling to (e^-u) states is 168 GeV, and for right-handed coupling is 176 GeV. Table 3 also gives mass limits at 95% confidence for a sample of other possible scalar leptoquark states.

Acknowledgements

We thank the DESY Directorate for their strong support and encouragement. The experiment was made possible by the inventiveness and the diligent efforts of the HERA machine group who succeeded in making HERA run in a very short time.

This work has been supported by the Natural Sciences and Engineering Research Council and the FCAR of Quebec, Canada, by the German Federal Ministry for Research and Technology (BMFT), by the Deutsche Forschungsgemeinschaft (DFG), by the Italian National Institute for Nuclear Physics (INFN), by the Japanese Ministry of Education, Science and Culture (the Monbusho) and its grants for Scientific Research, by the Netherlands Foundation for Research on Matter (FOM), by the Polish Government and Ministry of Education Research Programs, by the Spanish Ministry of Education and Science through funds provided by CICYT, by the UK Science and Engineering Research Council, by the MINERVA Foundation, by the Israel Ministry of Energy, by the German Israeli Foundation, by the US Department of Energy and by the US National Science Foundation.

Useful and informative conversations with Professors Barbara Schrempp and Erick Weinberg are gratefully acknowledged.

References

[1] J. C. Pati and A. Salam, Phys. Rev. Lett. 31 (1975) 661; Phys. Rev. D 10 (1974) 275.
H. Georgi and S. Glashow, Phys. Rev. Lett. 32 (1974) 438.
J. L. Hewett and T. G. Rizzo, Phys. Reports 183 (1989) 193.
R. J. Cashmore et al., Phys. Reports 122 (1985) 275.
W. Buchmüller, Schladming Lectures Suppl. XXVII (1985) 517 and references therein.

[2] W. Buchmüller et al., Phys. Lett. B191 (1987) 442.

[3] B. Schrempp, Proc. of Workshop on Physics at HERA Vol. 2 (DESY, 1992) 1034.

[4] W. Buchmüller and D. Wyler, Phys. Lett. B177 (1986) 377.

[5] OPAL Collab., M. Akrawy et al., Phys. Lett. B263 (1991) 123.
L3 Collab., B. Adeva et al., Phys. Lett. B261 (1991) 169.
DELPHI Collab., P. Abreu et al., Phys. Lett. B275 (1991) 222.
ALEPH Collab., D. DeCamp et al., Phys. Rep. 216 (1992) 253.

[6] UA2 Collab., J. Alitti et al., Phys. Lett. B274 (1992) 507.

[7] CDF Collab., S. Moulding et al., presentation at the Seventh Meeting of the American Physical Society (DPF) Fermilab (November 1992).

[8] Presentations by F. Eisele, B. Löhr, and B. Wiik, at Intern. Conf. on High Energy Physics (Dallas, August 1992).

[9] ZEUS Collab., M. Derrick et al., submitted to Phys. Lett.

[10] ZEUS Collab., M. Derrick et al., Phys. Lett. B297 (1992) 404.

[11] ZEUS Collab., M. Derrick et al., Phys. Lett. B293 (1992) 465.

[12] A. Caldwell et al., Nucl. Inst. and Meth. A321 (1992) 356.

[13] A. Andresen et al., Nucl. Inst. and Meth. A309 (1991) 101.

[14] A. Bernstein et al., to be submitted to Nucl. Inst. and Meth.
U. Mallik, Proc. of International Conference on High Energy Phyiscs, Fermilab(1990).

[15] N. Harnew et al., Nucl. Inst. and Meth. A279 (1989) 290.
B. Foster et al., Proc. of 3rd International Conf. on Advanced Technology and Particle Physics, Villa Omo, Como (1992), Oxford Univ. preprint OUNP-92-14, Nucl. Inst. and Meth. (to be published).

[16] S. Bentvelsen et al., Proc. of Workshop on Physics at HERA Vol. 1 (DESY, 1992) 23.

[17] H.-U. Bengtsson and T. Sjöstrand, Comp. Phys. Comm. 46 (1987) 43.
T. Sjöstrand, Proc. of Workshop on Physics at HERA Vol. 3 (DESY, 1992) 1405.

[18] J. G. Morfin and W. K. Tung, Z. Phys. C52 (1991) 13.

[19] D. Gingrich, University of Oxford preprint OUNP-92-19.
D. Gingrich and N. Harnew, Proc. of Workshop on Physics at HERA Vol. 3 (DESY, 1992) 1542.

[20] R. Brun et al., CERN DD/EE/84-1 (1987).

[21] See e.g. M. Aguilar-Benitez et al., Particle Properties Data Book (April 1990) 149 and Phys. Lett. B239 (1990).

[22] A. D. Martin et al., Durham/RAL preprint, DTP-92-16 and RAL-92-021, accepted for publication in Phys. Rev.

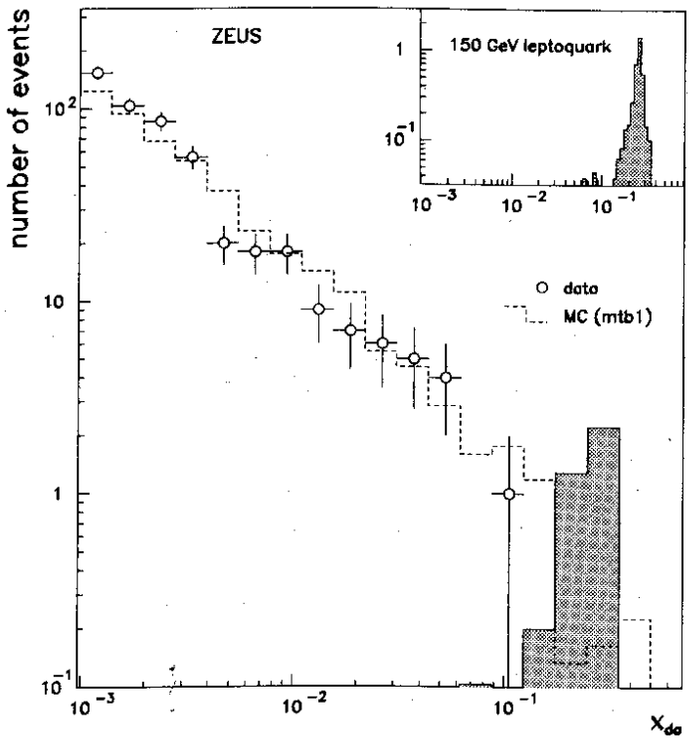

Figure 1: *Distribution in x_{DA} of the 465 events with $x_{DA} > .001$ in the final NC search sample (1659 candidates) . The data (circles) are shown with statistical error bars. The Monte Carlo prediction, normalized to the data luminosity, is shown as the open dashed histogram. The shaded histogram at $x_{DA} \approx 0.25$ corresponds to the expected signal from a leptoquark of mass $M_{LQ} = 150$ GeV with electroweak coupling. The same distribution on an expanded scale is shown in the inset at the upper right of the figure.*

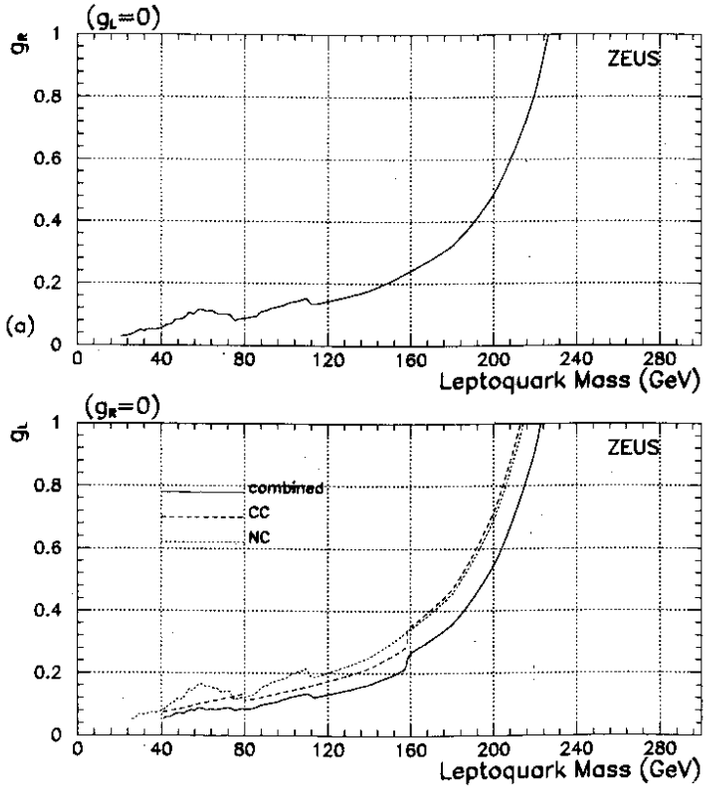

Figure 2: *The 95% confidence upper limits on the couplings of scalar leptoquarks with zero weak isospin and fermion number $F = -2$ versus the leptoquark mass in GeV. (a) The right-handed coupling limit from the NC decay mode with $b = 1$. (b) Assuming $b = \frac{1}{2}$, the left-handed coupling calculated from the NC data sample (dotted), from the CC data sample (dashed), and from the combined samples (solid).*
To obtain the limit for other branching fraction assumptions, the ordinate of the NC (CC) curve should be multiplied by

$$\sqrt{\frac{0.5}{b}} \quad \left(\sqrt{\frac{0.5}{1-b}}\right).$$

Because the limits from NC and CC are similar at larger masses, the combined left-handed coupling limit at large mass is largely independent of b.

A Appendix

The table below gives the 95% confidence limits on σ_{NC} and σ_{CC}, the cross-sections times branching ratios, respectively, for production and decay of resonant states into $e + jet$ and $\nu + jet$, as a function of the mass of the state, M_{LQ}.

$M_{LQ}(GeV)$	$\sigma_{NC}(nb)$	$\sigma_{CC}(nb)$	$M_{LQ}(GeV)$	$\sigma_{NC}(nb)$	$\sigma_{CC}(nb)$
25.	0.368	—	155.	0.228	0.167
30.	0.539	—	160.	0.231	0.168
35.	0.482	—	165.	0.233	0.170
40.	0.341	—	170.	0.236	0.172
45.	0.411	—	175.	0.239	0.173
50.	0.455	0.275	180.	0.242	0.175
55.	0.611	0.268	185.	0.245	0.178
60.	0.608	0.261	190.	0.248	0.266
65.	0.473	0.255	195.	0.252	0.270
70.	0.365	0.250	200.	0.256	0.275
75.	0.208	0.245	205.	0.260	0.280
80.	0.209	0.241	210.	0.265	0.285
85.	0.209	0.238	215.	0.270	0.291
90.	0.258	0.165	220.	0.275	0.296
95.	0.280	0.164	225.	0.280	0.302
100.	0.281	0.163	230.	0.286	0.308
105.	0.302	0.163	235.	0.293	0.315
110.	0.303	0.162	240.	0.300	0.323
115.	0.215	0.162	245.	0.307	0.311
120.	0.216	0.162	250.	0.315	0.339
125.	0.217	0.162	255.	0.324	0.347
130.	0.219	0.163	260.	0.333	0.356
135.	0.220	0.163	265.	0.343	0.364
140.	0.222	0.164	270.	0.354	0.373
145.	0.224	0.165	275.	0.366	0.383
150.	0.226	0.166	280.	0.380	0.392